Mapping Stiffness Perception in the Brain with an fMRI-Compatible Particle-Jamming Haptic Interface

Samir Menon[1], Andrew A. Stanley[2], Jack Zhu[1], Allison M. Okamura[2], and Oussama Khatib[1]

***Abstract*— We demonstrate reliable neural responses to changes in haptic stiffness perception using a functional magnetic resonance imaging (fMRI) compatible particle-jamming haptic interface. Our haptic interface consists of a silicone tactile surface whose stiffness we can control by modulating air-pressure in a sub-surface pouch of coarsely ground particles. The particles jam together as the pressure decreases, which stiffens the surface. During fMRI acquisition, subjects performed a *constant probing* task, which involved continuous contact between the index fingertip and the interface and rhythmic increases and decreases in fingertip force (1.6 Hz) to probe stiffness. Without notifying subjects, we randomly switched the interface's stiffness (switch time, 300–500 ms) from soft (200 N/m) to hard (1400 N/m). Our experiment design's constant motor activity and cutaneous tactile sensation helped disassociate neural activation for both from stiffness perception, which helped localized it to a narrow region in somatosensory cortex near the supra-marginal gyrus. Testing different models of neural activation, we found that assuming indepedent stiffness-change responses at both soft-hard and hard-soft transitions provides the best explanation for observed fMRI measurements (three subjects; nine four-minute scan runs each). Furthermore, we found that neural activation related to stiffness-change and absolute stiffness can be localized to adjacent but disparate anatomical locations. We also show that classical finger-tapping experiments activate a swath of cortex and are not suitable for localizing stiffness perception. Our results demonstrate that decorrelating motor and sensory neural activation is essential for characterizing somatosensory cortex, and establish particle-jamming haptics as an attractive low-cost method for fMRI experiments.**

I. Introduction

Decorrelating human somatosensory perception from motor control during fMRI experiments is complicated by the latter's slow measurements of haemodynamic responses to neural activation [1], [2]. While past research has extensively studied somatosensory perception [3], [4], [5], [6], [7], [8], it remains a challenge to rapidly and reliably localize somatosensory neural activation to precise anatomical locations for individual subjects. A major problem that experimenters face is that the constrained MRI workspace limits motions and disallows tools that can precisely control task onset, duration, and offset. Combining fMRI with controllable haptic interfaces promises to overcome this problem, provided such interfaces are cost effective, easy to operate, and induce no imaging artifacts.

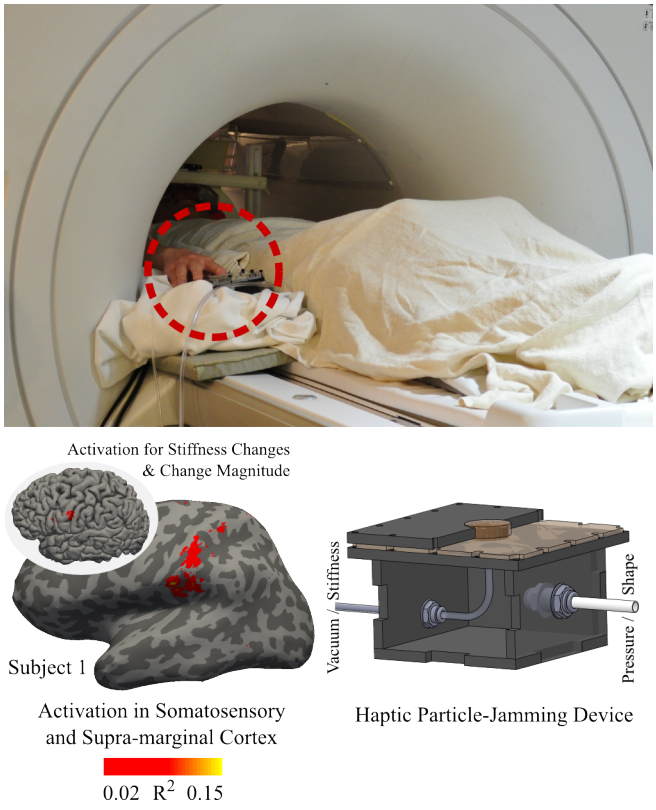

Fig. 1. Localizing Stiffness-Change in the Brain. An fMRI-compatible haptic particle-jamming device A constant probe stiffness perception task localized neural activation to somatosensory, using our particle-jamming haptic interface, which randomly switched between soft and hard states. The experiment reliably activated somatosensory and supramarginal cortex. Coefficient of determination shown for a general linear model that assumed somatosensory responses.

Attempts to engineer haptic interfaces that can study human somatosensory perception with fMRI have primarily focused on avoiding electromechanical actuators and sensors. One such approach placed a haptic interface's actuators outside the MRI scan room and used a hydrostatic transmission to control a slave device near the scanner [9]. Alternative designs use pneumatics to power haptic manipulandums [10], [11]. Yet other strategies have involved shielding electromagnetic components that are located inside the scanner room [12], [13]; designing mechanisms to extend the reach of commercial haptic devices outside of the MRI field [14]; and building devices from MRI-compatible polymers that can be actuated via wires from the control room [15]. While

*This work was supported by a Stanford University BioX fellowship (S. Menon) and a Stanford University BioX Neuroventures Research Grant (O. Khatib)

[1]S. Menon, J. Zhu, and O. Khatib are with the Artificial Intelligence Laboratory, Department of Computer Science, Stanford University, Stanford, CA 94305, USA smenon@stanford.edu, jackzhu@stanford.edu, ok@cs.stanford.edu

[2]A. A. Stanley and A. M. Okamura are with the Department of Mechanical Engineering, Stanford University, Stanford, CA 94305, USA astan@stanford.edu, aokamura@stanford.edu

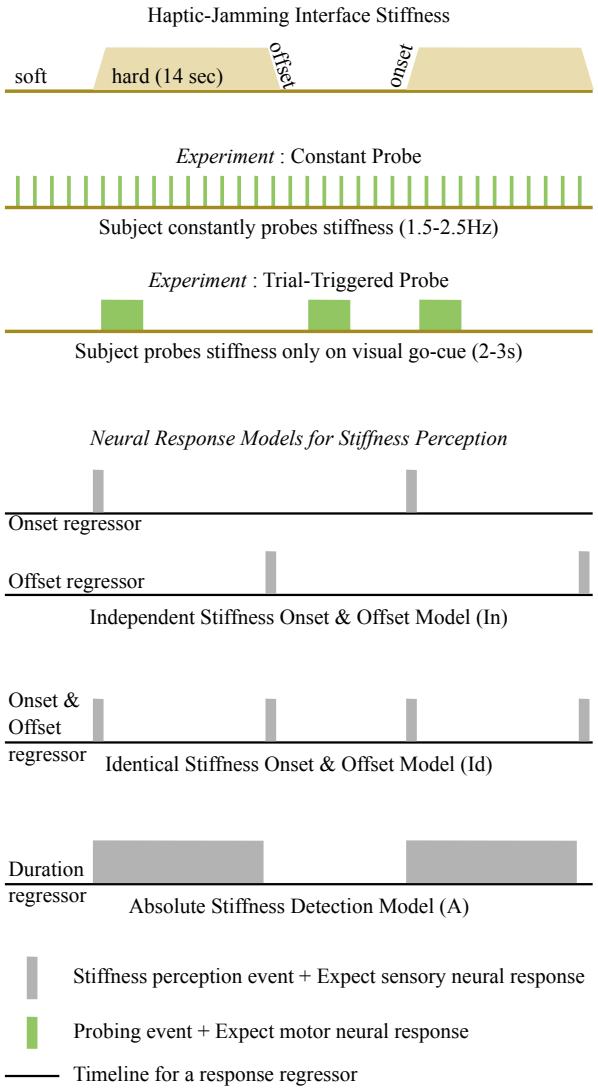

Fig. 2. Experiment Design and Neural Activation Models. We designed two experiments to map stiffness perception using fMRI. A *constant probe* experiment required subjects to constantly probe the haptic jamming device's stiffness, which changed randomly between a soft and a hard state (see top; yellow timeline). A second *trial-triggered probe* experiment provided a visual cue to probe stiffness at random points of time. Three response models were used to explain the resulting neural activation in subject brains (black timeline). The models explain transient neural activation at soft-hard and hard-soft transitions (*In, Id*), or steady-state activation increases that correlate with absolute stiffness (*A*). Note that the absolute model's duration is shown for the constant probe condition; for the trial-triggered probe, the duration matches the probe's duration (green block above)

shielding can be effective [13], avoiding electromagnetic components simplifies device design, reduces cost, and ensures compatibility with a wide variety of scanning protocols.

This paper presents a novel fMRI-compatible haptic interface to study how stiffness perception at human fingertips maps on to the brain (Fig. 1). The device uses particle-jamming [16] to modulate the stiffness of a tactile surface. The surface is made of flexible membrane filled with a granular material, which can be rapidly switched between being soft or rigid by modulating air pressure. Leveraging the interface, we developed a novel experiment that involves a repetitive probing motor task combined with randomized changes in interface stuffness, which decorrelates stiffness perception from motor and other sensory inputs. Our experiment helped us localize neural activation due to absolute stiffness changes as well as stiffness change transients to anatomically adjacent but separate parts of the brain. We also demonstrate that classical finger-tapping block design experiments are unsuitable to study stiffness perception since they correlate numerous planning, motor and sensory cues, which dominate neural activation due to stiffness perception. Finally, we show that our haptic interface does not induce noise in fMRI measurements, which sets the stage for future experiments to map somatosensory neural activation in the human brain.

II. Modeling Neural Activation for Stiffness Perception

We used a *constant probing* protocol to test whether controlled stiffness-changes could elicit reliable neural activation in somatosensory brain regions (Fig. 2). We adopted a simple approach to factorize out neural activation related to motor control and tactile perception—we kept both constantly active through entire experiment runs (see Appendix. *Experiment Protocol: Constant probe*). The only transient stimuli were due to changes in tactile stiffness. Subjects received no visual or auditory cue and only focused on maintaining a constant probing frequency at the fingertip without breaking contact.

To simplify the experiment and negate the possibility of any electronics related imaging artifacts, we did not monitor probing motions inside the MRI scanner. Instead, we recorded each subject's probe timing statistics outside the scanner after the experiment was over (Fig. 3). Subjects were instructed to maintain fingertip probing patterns that were similar to those within the MRI during the experiment. Two out of three subjects were highly reliable, while the third exhibited a linear drift, which is unlikely to interfere with subsequent fMRI analyses since its effects can be segregated using a noise regressor.

We analyzed our data using three different neural response models, each of which made different assumptions about the underlying neural activation patterns (see Fig. 2). Comparing each model's explanatory power and ability to localize responses to unique brain regions can provide insights into the nature of underlying neural sensory processing. We convolved each model's regressors with a canonical haemodynamic response function to accommodate the fact that fMRI measures magnetic field fluctuations due to neuron-metabolism induced blood oxygenation changes [1], [2]. We also regressed noise using the principal time series components of brain voxels (cubic pixels) that were unresponsive to our task specification [17] (using GLMDenoise; see Appendix. *fMRI Analysis*). Finally, we anatomically localized voxels based on how well their neural activation was explained by our models.

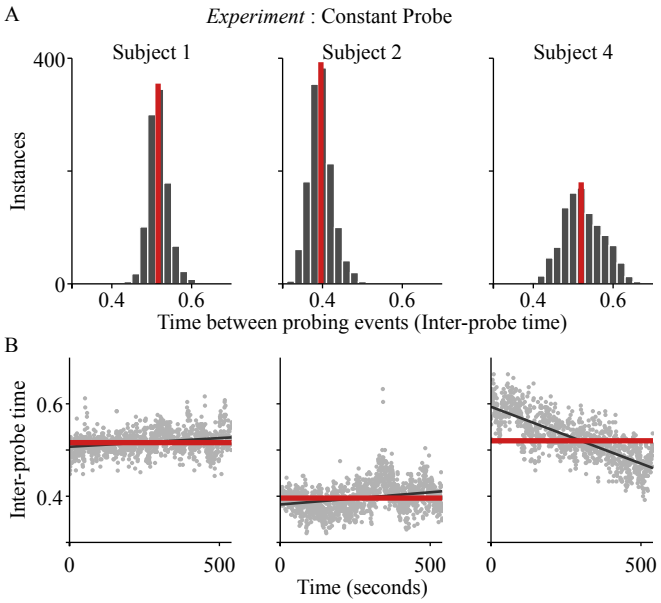

Fig. 3. Constant Probe Performance. Subjects' probing patterns, measured outside the MRI after the experiment. A. Tapping histograms for subjects were unimodal. Distribution medians shown in red. B. Two subjects maintained consistent inter-probe timing, while one subject exhibitied a linear drift. Median values are shown in red, and regression lines are shown in black.

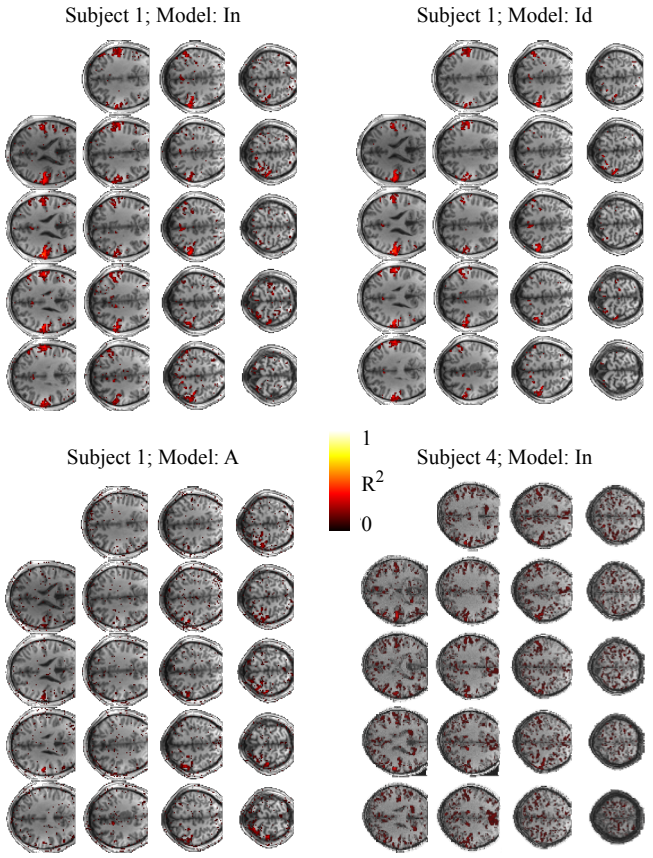

Fig. 4. Model Reliability Across the Brain. Stiffness-change detector models (*In, Id*) explained neural variance in different anatomical regions when compared to the steady-state activation model (*A*). The independent response model's extra degree-of-freedom helped it explain neural activation in more brain voxels than the identical response model. Coefficients of determination (R^2) were computed for each voxel by combining variance explained across all scan runs.

A. Model: Independent Stiffness Onset & Offset

Our first model assumed independent neural activation that coincided with the soft-hard and hard-soft stiffness transitions (In, see Fig. 2). This model required stereotypical neural responses for a given transition type, with potentially different responses for the other transition type. Assuming independent responses enabled the model to capture potential motor control related activation at the transitions, which helps provide a baseline for other models. A robust experiment should completely decorrelate motor responses and make sure that this model's explanatory power and anatomical localization match any other stiffness-change detection model with similar stiffness-event triggers and degrees-of-freedom.

B. Model: Identical Stiffness Onset & Offset

Our second model assumed identical neural activation at the soft-hard and hard-soft stiffness transitions (Id, see Fig. 2). This model required stereotypical neural responses for both transition types, which conservatively assumes neural activation due to stiffness perception has a single dimension. This model is more likely to underfit the data than overfit it. We expected this model's ability to explain neural activation to be lower than, and it's anatomical localization to be a subset of, the independent model.

C. Model: Absolute Stiffness Detection

Our third model matched classical block designs that assume different steady-state neural activation when the haptic interface's stiffness was either soft or hard (A, see Fig. 2). This model's steady state activity assumption, however, segregates it from the other models. Like *Id*, it conservatively assumes a single neural stiffness dimension, and is likely to underfit the data.

This model's predictions can help establish a baseline to compare past research [18] with our results. Moreover, obtaining disparate anatomical localization with this model—when compared to stiffness-change models—would indicate that different parts of the brain represent stiffness perception transients and steady-state responses.

III. Neural Activation in Individual Subjects

Regressing our sensory perception models against neural activation predicted that somatosensory and supra-marginal cortex respond to stiffness perception at the index fingertip (Fig. 4). The independent response model explained variance in the most voxels. The identical response model underfit the data and did not explain variance in as many voxels. These results support the hypothesis that soft-hard and hard-soft transitions are represented in the same anatomical location, but have potentially different underlying activity patterns at the individual neuron level. The absolute response model, in addition, mapped to a different set of voxels than the

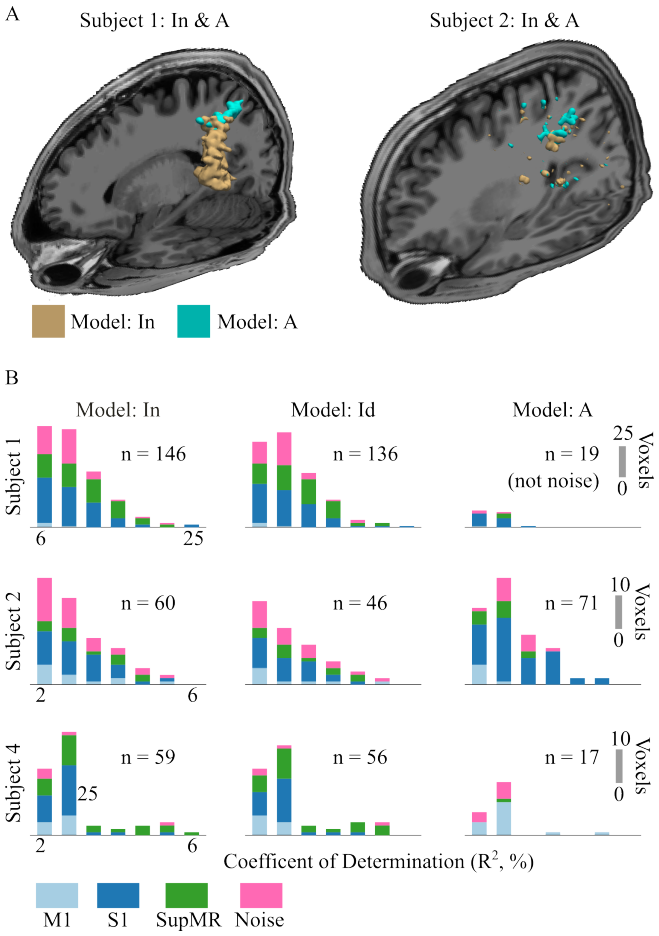

Fig. 5. Model Explanatory Power by Anatomical Region. A. A volumetric rendering shows voxels whose neural activation time series was explained by the independent and absolute models ($R^2 > 5\%$ shown). The voxels are near the point where somatosensory and supra-marginal cortex meet. Both stiffness-change detector models (*In, Id*) mapped to similar voxels (not shown), and were anatomically inferior to the absolute model's voxels with a limited region of overlap. Model localization to anatomical regions were similar for a second subject (right). B. R^2 distribution histograms show the models' explanatory power across somatosensory, supra-marginal, and primary motor cortex for all three subjects. The number of white-matter voxels fitted by a model provided a noise metric.

other two models (superior in the cortex), supporting the hypothesis that different parts of the brain represent steady-state stiffness responses and stiffness-change transients.

We used volumetric rendering to visualize anatomical overlap between the independent change detector and the absolute magnitude detector models (Fig. 5). Both change detector models mapped to similar regions (not visualized), so we compared how well they explain neural activation within their shared region instead. The absolute response model, interestingly, explained neural activation in a separate anatomical region (superior; partial overlap with others).

IV. Contrasting Model Explanatory Power

Given that our anatomical visualization revealed no differences between change detector models, we proceeded to compare how well they explain neural activation variance in somatosensory, supra-marginal and primary motor cortex

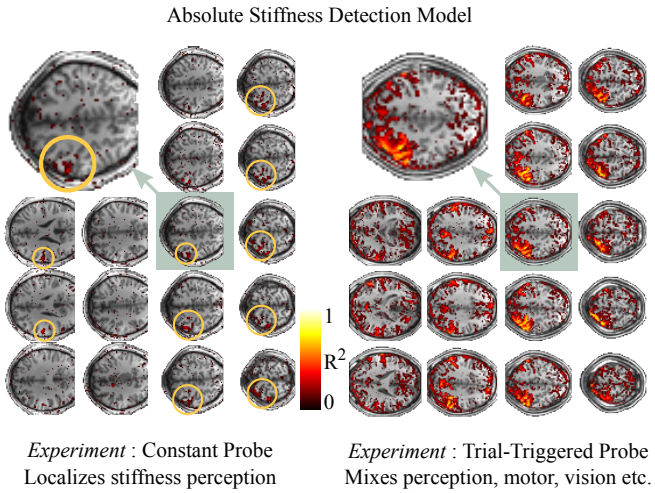

Fig. 6. Decorrelating Motor Responses. The trial-triggered probe experiment protocol (right) elicited widespread neural activation (subject 3). Associated anatomical locations include canonical motor regions, which suggests that trial-triggered finger-tapping is not suitable to study stiffness perception. In contrast, the constant probe protocol (left) effectively decorrelated motor responses and confined neural activation to small focused regions (encircled; subject 1).

(see Fig. 5.B). We found that the independent model explained more variance than the identical model for two out of three subjects (see Fig. 5.B; counts indicate grey matter voxels), which confirms observations made by looking at the model's slice-by-slice R^2 distribution shown earlier. This was expected, since the independent model has one more degree-of-freedom. Surprisingly, the independent model's noise characteristics were similar to the identical model. This suggests that that the independent model is superior, and that fMRI's haemodynamic responses capture high frequency neural activation differences at times when stiffness increases and decreases.

Compared to the independent (change detector) model, the absolute model explained variance in fewer voxels for two subjects, and explained a roughly similar number of voxels in one. It is noteworthy that the variance explained was lower for the second and third subjects, when compared to the first subject. This warrants further investigation.

While our results are promising and consistent with past research [18], generalizing them requires extensive experimentation across multiple subjects. For now, these results should primarily be interpreted as a demonstration of particle-jamming haptics to characterize the neural correlates of human sensory perception.

V. Dissociating Motor and Sensory Neural Responses

As a control, we compared our experiment design with a trial-triggered probe task. The control experiment used a simple and classical design to study neural activation due to absolute stiffness: repeatable blocks of activity with randomized delays between them. Subjects started with their hands at rest. They placed their index finger just above the haptic interface's surface after a visual plan cue. A probe

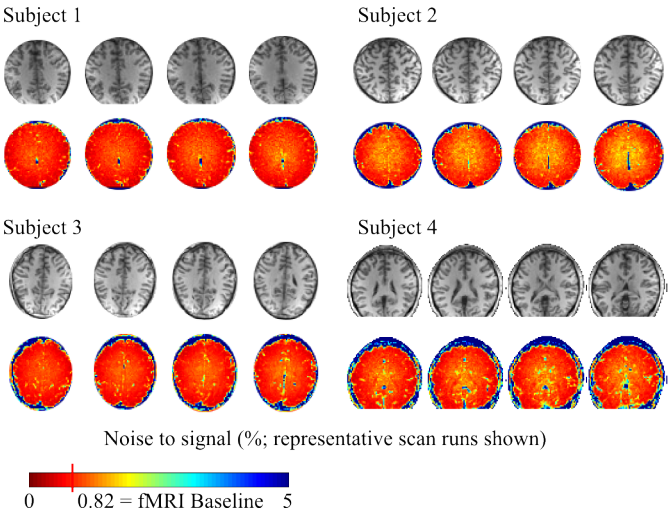

Fig. 7. fMRI Temporal Noise to Signal. Our fMRI protocol, non-metallic haptic interface construction, and pneumatic particle-jamming control helped maintain temporal noise-to-signal near the scanner's baseline noise (human brain; resting-state).

visual cue then instructed subjects to slowly press down on the surface twice to estimate its stiffness. We simultaneously measured neural activation with fMRI.

The trial-triggered experiment elicited neural activation across a surprisingly large swath of cortex, including canonical motor regions (Fig. 6). We attribute this to a large degree of sensory deprivation during the experiment, followed by a task that first provides visual input, next requires decision making and motor control, and finally results in somatosensory perception. Moreover, somatosensory responses were uncontrolled and had the potential to be irregular and different each time, which could elicit network-level activity across more cortical regions. Our constant finger probe experiment, in contrast, relied on no event-related visual stimulus, decision making, or motor task, which was critical for our neural activation models to localize stiffness perception within the brain's somatosensory regions.

VI. Conclusion

Our demonstration that simple low-cost particle-jamming haptic devices can effectively map human somatosensory perception provides a promising new technique for neuroimaging experiments. Our haptic framework's operating simplicity, lack of fMRI measurement noise (Fig. 7), and non-metallic construction make it fMRI-compatible and easy to integrate with existing pipelines. Moreover, the device uses commonly available materials and fabrication techniques, making it straightforward to adopt. In addition, our results suggest that somatosensory neuroimaging studies should adopt controlled experiments that decouple neural activation due to motor control or cutaneous inputs. Our experiment design offers one such protocol, and it is straightforward to generalize its principles to more complex haptic experiments with potentially numerous degrees-of-freedom.

To end, we note a decrease in overall explanatory power in the constant probe experiment when compared to the trial-triggered probe. This may be interpreted in numerous ways. For instance, stiffness perception at the fingertip could be anatomically localized in the brain, but the brain might primarily represent only stiffness-change. This would reduce the explanatory power of an absolute stiffness model. Alternatively, the stiffness levels supported by the particle-jamming haptic device might be insufficient to elicit a steady-state response. Finally, the motor representation could be distributed and might overlap with the sensory representation. Given that our models only attempt to explain sensory activation, the constant probing activity could be constantly injecting noise that remains unaccounted for. Factorizing such sensory-motor representation overlap into its constituents is a logical next step.

Appendix

Particle-Jamming Haptic Interface

The controllable stiffness device consists of a hollow cylindrical shell of silicone filled with coffee grounds that clamps over a pressure-regulated air chamber. The cylindrical cell measures 1 inch in diameter and 5/16 inches thick with an additional layer of silicone outside the bottom that serves as a a seal when clamped between the two layers of acrylic that form the top of the chamber. The layer of acrylic that the silicone sits on top of includes a circular cutout the size of the cell diameter such that the cell itself is suspended above the air chamber. A syringe connects to the bottom of the silicone at the center of the cell via a tube that runs through the air chamber so that pulling 50 mL of air from the interior of the silicone generates 15 inHg of vacuum to jam the coffee grounds together. From experiments in prior work with the device [19], 15 inHg of vacuum provides a stiffness of 1400 N/m compared to 200 N/m when no vacuum is applied. Increasing the pressure in the chamber while the cell is in its soft state causes the cell to balloon outward. In this study, the pressure was held at a constant 0.6 psi to maintain the cell shape while the user interacted with it, consistent with the techniques used in psychophysical studies performed with the device [19]. The silicone is Ecoflex 00-30 rubber (Smooth-On, Inc., Easton, PA), which has a 100% Modulus of 10 psig and a 900% elongation at break, and the construction of this device is described in much greater detail in [16]. By design, the device is fMRI-compatible [20].

Experiment Protocol: Constant probe

Each experiment session included nine runs. Each run was two hundred and forty five seconds long. During each run, subjects kept their right hand's index fingertip on the haptic jamming device's surface, and periodically (1.5–2.5Hz) probed surface stiffness by gently pushing harder against it. An operator randomly changed the device's stiffness (switch time, 300–500ms) between the hard (1400N/m) and soft states (200N/m). Subjects received no information about the stiffness-change apart from tactile perception at their finger. The protocol thus decorrelated motion and touch perception (constant) from stiffness perception (controlled and randomized). All subjects executed one practice run inside the MRI scanner before the actual scanning experiment.

Experiment Protocol: Trial-triggered probe

Subjects received task instructions by looking at a monitor. They started at rest (*Rest* cue; red), were asked to plan a pressing motion (*Plan* cue; blue), executed two presses with a randomized particle-jamming stiffness (*Execute* cue; green), and finally returned to the initial rest position. Each subject executed twenty three presses (x2 finger taps per press) for the soft and stiff conditions in each fMRI scan run, and executed four runs during the scan session.

fMRI Scans and Pre-processing

All fMRI scans were conducted at Stanford University's Center for Cognitive and Neurobiological Imaging on a GE Discovery MR750 3 Tesla MRI scanner, with a 32 channel Nova Medical head coil. The scan protocol was gradient echo EPI with a 16cm field of view sampled at a 64×64 resolution ($2.5\times2.5\times2.5\text{mm}^3$ voxels), a 1.57s repetition time, a 28ms echo time, and a 72^o flip angle. All scan runs were preceeded by 2^{nd}-order polynomial shimming and were sandwiched by spiral fieldmap scans ($2.5\times2.5\times5\text{mm}^3$ voxels). After scanning, the fMRI images were slice time corrected, motion corrected (SPM), spatially undistorted using fieldmaps, and analyzed to compute temporal noise-to-signal (as in [13]).

fMRI Analysis

Voxel reliability (R^2) values were computed using GLMdenoise [17], with an assumed canonical haemodynamic response. Different stiffness response models required different stimulus design specifications, and thus their R^2 scores were computed independent of each other. Cortical segmentation used Freesurfer's Desikan–Killiany atlas [21]. All volumetric images were plotted using freeview, which smoothed the rendered surface plots (2 steps).

Human Subjects

Subjects were healthy right-handed males with no history of motor disorders: S1, 19y, 170lb, 6'2"; S2, 20y, 153lb, 5'9"; S3, 23y, 120lb, 5'5"; S4, 22y, 120lb, 5'6". S1, S2, and S4 performed the constant probe task. S3 performed the trial-triggered probe task. All subjects gave their informed consent in advance on a protocol approved by the Institutional Review Board (IRB) at Stanford University.

Head Motion

Subjects used a bite-bar with a custom dental dam to minimize head motion during all scan runs, including the practice run. Head motion levels were $<$0.1mm between scan volumes and $<$1mm over the duration of any scan run.

ACKNOWLEDGMENT

We acknowledge Francois Conti's comments on experiment design and Hari Ganti's assistance with data collection. We thank Kendrick Kay, Laima Baltusis and Robert Dougherty for helping develop fMRI protocols.

REFERENCES

[1] N. K. Logothetis and B. A. Wandell, "Interpreting the bold signal," *Annu. Rev. Physiol.*, vol. 66, pp. 735–769, 2004.

[2] N. K. Logothetis, "What we can do and what we cannot do with fmri," *Nature*, vol. 453, no. 7197, pp. 869–878, Jun 2008.

[3] P. A. Gelnar, B. R. Krauss, P. R. Sheehe, N. M. Szeverenyi, and A. Apkarian, "A comparative fmri study of cortical representations for thermal painful, vibrotactile, and motor performance tasks," *NeuroImage*, vol. 10, no. 4, pp. 460 – 482, 1999.

[4] G. Robles-De-La-Torre and V. Hayward, "Force can overcome object geometry in the perception of shape through active touch," *Nature*, vol. 412, pp. 0028–0836, 2001.

[5] H. Olausson, Y. Lamarre, H. Backlund, C. Morin, B. Wallin, G. Starck, S. Ekholm, I. Strigo, K. Worsley, A. Vallbo, and M. Bushnell, "Unmyelinated tactile afferents signal touch and project to insular cortex," *Nature Neuroscience*, vol. 5, pp. 1097–6256, 2002.

[6] C. L. Reed, R. L. Klatzky, and E. Halgren, "What vs. where in touch: an fmri study," *NeuroImage*, vol. 25, no. 3, pp. 718 – 726, 2005.

[7] S. Lederman and R. Klatzky, "Haptic perception: A tutorial," *Attention, Perception, & Psychophysics*, vol. 71, no. 7, pp. 1439–1459, 2009.

[8] D. Rosenbaum, *Human motor control*. Academic Press, 2009.

[9] R. Gassert, L. Dovat, O. Lambercy, Y. Ruffieux, D. Chapuis, G. Ganesh, E. Burdet, and H. Bleuler, "A 2-dof fmri compatible haptic interface to investigate the neural control of arm movements," in *Proceedings of the IEEE International Conference on Robotics and Automation*. IEEE, 2006, pp. 3825–3831.

[10] J. Diedrichsen, Y. Hashambhoy, T. Rane, and R. Shadmehr, "Neural correlates of reach errors," *The Journal of Neuroscience*, vol. 25, no. 43, pp. 9919–9931, 2005.

[11] N. Y., C. Hollnagel, A. Blickenstorfer, S. S. Kollias, and R. Riener, "Comparison of mri-compatible mechatronic systems with hydrodynamic and pneumatic actuation," *Mechatronics, IEEE/ASME Transactions on*, vol. 13, no. 3, pp. 268–277, June 2008.

[12] S. Li, A. Frisoli, L. Borelli, M. Bergamasco, M. Raabe, and M. Greenlee, "Design of a new fmri compatible haptic interface," in *EuroHaptics conference, and Symposium on Haptic Interfaces for Virtual Environment and Teleoperator Systems. World Haptics*, March 2009, pp. 535–540.

[13] S. Menon, G. Brantner, C. Aholt, K. Kay, and O. Khatib, "Haptic fMRI : Combining functional neuroimaging with haptics for studying the brain's motor control representation," in *Proceedings of the 13th Annual Conference of the IEEE Engineering in Medicine and Biology Society*, July 2013, pp. 4137–42.

[14] A. Hribar, M. Munih, and B. Koritnik, "fmri compatible haptic interface system," in *Proceedings of the IEEE International Conference on Robotics and Biomimetics*, Feb 2009, pp. 318–323.

[15] U. Spaelter, D. Chapuis, R. Gassert, R. Moser, and H. Bleuler, "A versatile mri/fmri compatible spherical 2-dof haptic interface," in *Proceedings of the IEEE/RAS-EMBS International Conference on Biomedical Robotics and Biomechatronics*, Feb 2006, pp. 727–732.

[16] A. A. Stanley, J. C. Gwilliam, and A. M. Okamura, "Haptic jamming: A deformable geometry, variable stiffness tactile display using pneumatics and particle jamming," in *IEEE World Haptics Conference*, 2013, pp. 25–30.

[17] K. Kay, A. Rokem, J. Winawer, R. Dougherty, and B. Wandell, "Glmdenoise: a fast, automated technique for denoising task-based fmri data," *Frontiers in Neuroscience*, vol. 7, no. 247, 2013.

[18] R. S. Johansson and J. R. Flanagan, "Coding and use of tactile signals from the fingertips in object manipulation tasks." *Nature reviews. Neuroscience*, vol. 10, no. 5, pp. 345–59, May 2009.

[19] A. M. Genecov, A. A. Stanley, and A. M. Okamura, "Perception of a Haptic Jamming Display : Just Noticeable Differences in Stiffness and Geometry," in *IEEE Haptics Symposium*, 2014, pp. 333–338.

[20] R. Gassert, E. Burdet, and K. Chinzei, "Mri-compatible robotics," *Engineering in Medicine and Biology Magazine, IEEE*, vol. 27, no. 3, pp. 12–14, 2008.

[21] R. S. Desikan and R. J. e. a. Killiany, "An automated labeling system for subdividing the human cerebral cortex on mri scans into gyral based regions of interest," *NeuroImage*, vol. 31, no. 3, pp. 968 – 980, 2006.